Geophysical Journal International

Geophys. J. Int. (2010) **181,** 756–761 doi: 10.1111/j.1365-246X.2010.04566.x

Magnetic properties and anisotropy constant of goethite single crystals at saturating high fields

F. Martin-Hernandez[1] and M. M. García-Hernández[2]

[1] *Department of Geophysics, Faculty of Physics, Complutense University,* E-28040 *Madrid, Spain. E-mail: fatima@fis.ucm.es*
[2] *Instituto de Ciencia de Materiales de Madrid (CSIC), Cantoblanco,* E-28049 *Madrid, Spain*

Accepted 2010 February 14. Received 2010 February 1; in original form 2009 November 27

SUMMARY

The applied fields in previous studies of goethite's magnetic properties were often not sufficiently high to reach reversible magnetization behaviour of the hard magnetic iron oxide (α-FeOOH). Existing data of its magnetic anisotropy constant are fairly scattered that hampers the further development of more elaborate models of remanence acquisition, magnetic susceptibility behaviour or trends in microcoercivity. Classic rock magnetic properties (magnetization of remanence M_r, saturation magnetization M_s and coercive force B_c) and the first anisotropy constant K on six goethite natural crystals have been determined at room and low temperature using hysteresis up to 9 T. After a detailed analysis of the magnetic properties of the samples, a mean value of $K = 90 \pm 20$ Jm^{-3} has been evaluated at room temperature and $K = 210 \pm 40$ Jm^{-3} at 5 K for pure goethite.

Key words: Magnetic fabrics and anisotropy; Magnetic mineralogy and petrology; Rock and mineral magnetism.

1 INTRODUCTION

Goethite is an antiferromagnetic iron-oxy-hydroxide (α-FeOOH) that crystallizes in the orthorhombic system. Goethite crystals are made out of smaller crystallites of which magnetic properties are coupled by the interaction between crystallites (Mørup 1990; Coey *et al.* 1995).

Over the last century, goethite has been identified in soils and sediments on Earth (e.g. Evans & Heller 2003) and on the Martian surface (Bibring *et al.* 2007). The presence and preservation of goethite is an indicator of the soil conditions of formation and/or burial history (Balsam *et al.* 2004). Additionally, it has been shown to carry a stable remanent magnetization often related to secondary processes such as weathering and therefore it can carry paleomagnetic stable directions of secondary character (e.g. Banerjee 1970; Dekkers & Rochette 1992; Özdemir & Dunlop 1996). Thus there is a strong interest in its magnetic and physical properties. The basic magnetic properties of synthetic and natural goethite have been studied in detail (Dekkers 1988; Dekkers 1989a, 1989b; Rochette & Fillion 1989; Dekkers 1990; Liu *et al.* 2006). However, the high magnetic fields required to reach reversible behaviour makes it difficult to evaluate coercivity and derived properties (Coey *et al.* 1995; Maher *et al.* 2004; Rochette *et al.* 2005).

Micromagnetic models, theories of acquisition of magnetic remanence or studies of orientation of magnetic particles require a precise evaluation of the first magnetic anisotropy constant (K). Most of the values reported for K in goethite particles have been determined by Mössbauer spectrometry at low temperatures from 4 to 80 K (Meagher *et al.* 1986; Pankhurst & Pollard 1990; Bocquet *et al.* 1992) and a few estimations at room temperature (Coey *et al.* 1995; Madsen *et al.* 2009). However, they are one order of magnitude higher than the only available values determined by magnetic techniques (Dekkers 1989b).

This work reports the first anisotropy constant of eleven goethite crystals by DC magnetometry techniques, using fields up to 9 T where the reversibility of the hysteresis loops has been observed. Samples have been measured along the crystallographic c-axis, which is the easy magnetization direction. The hysteresis loops are expected to resemble a square loop in a uniaxial magnetic model with the easy axes statistically oriented along the direction of measurement.

2 SAMPLES AND METHODS

Eleven samples from six different natural crystals of goethite from Morocco have been measured to determine the first anisotropy constant. The average size of the samples is about 2 cm in length. Crystals are elongated along the crystallographic c-axis, which is the direction of minimum susceptibility and confers goethite an inverse AMS fabric (Rochette *et al.* 1992; Özdemir & Dunlop 1996). Each crystal has been subdivided into two samples were magnetic hysteresis at two temperatures and low temperature remanence cycling have been carried out. Additionally, from each crystal, one small chip was cut to carry out thermomagnetic analysis. Also some mg of powder was prepared from which X-ray diffraction, Al, Ni, Co, Mn and Fe content based on mass spectrometry was determined at the Research Assistance Spectrometry Center from the UCM

Diffractograms were determined on a X'Pert MPD (Multi-Purpose Diffractometer manufactured by Philips) equipped with

Table 1. Compositonal analysis of the main cations Al, Fe, Co, Mn and Ni determined by mass spectrometry.

Sample name	Al (per cent)	Fe (per cent)	Co (μg g^{-1})	Mn (μg g^{-1})	Ni (μg g^{-1})	X-ray	T_N (K)	T_M (K)
GT-1	0.238 ± 0.010	61.7 ± 1.9	< 5.0	305 ± 15	<5.0	Gt and Hm	383	249
GT-2	0.346 ± 0.014	61.1 ± 1.8	< 5.0	174 ± 9	<5.0	Gt and Hm	380	197
GT-3	0.310 ± 0.012	61.3 ± 1.8	< 5.0	1249 ± 62	<5.0	Gt	353	
GT-4	0.271 ± 0.011	61.1 ± 1.8	< 5.0	790 ± 40	6.0 ± 0.6	Gt and Hm	375	257
GT-5	0.652 ± 0.026	55.1 ± 1.7	< 5.0	1444 ± 72	<5.0	Gt	392	
GT-7	0.384 ± 0.015	61.3 ± 1.8	< 5.0	355 ± 18	<5.0	Gt and Hm	372	197

Notes: Magnetic phases identified by X-ray diffraction where Gt denotes goethite and Hm denotes hematite, Néel temperature of the goethite phase (T_N) and Morin temperature of the hematite phase (T_M) when present.

a Cu-X-ray source (Kα1 = 1.54056 Å and Kα2 = 1.54439 Å). The diffractograms have been analysed with the X' Pert HighScore Plus software from PANalytical.

Al, Ni, Co, Mn and Fe content has been determined by ICP-OES mass spectrometry analysis in a Optima 3200 Dual manufactured by Perkin Elmer Mass. The samples have been digested by acid solution with no interference from acid in the solution.

Thermomagnetic analysis was performed on a Variable Force Translation Balance High-sensitivity Magnetometer (manufactured by Petersen Instrument). Samples were heated to 700 °C and cooled to room temperature in air at a rate of 10 °C min^{-1}. A field of 1 T was applied parallel to the crystallographic *c*-axis. The Néel temperature has been determined from the peak in the warming curve.

Hysteresis curves were determined at 300 and 5 K up to 9 T using a Physical Property Measurement System (PPMS) Magnetometer (manufactured by Quantum Design). The residual field of the instrument is always lower than 1.2 mT. Since a reversible state was reached between 3 and 4 T, some room-temperature hysteresis loops were measured up to 7 T to avoid unnecessarily forcing the instrument at the highest field. Remanent saturation magnetization (M_r) was calculated from the hysteresis loop as the magnetization at zero field (ZFC). Magnetization (M_s) and coercive force (B_c) were computed after high field slope correction. The first anisotropy constant of goethite has been computed according to a uniaxial anisotropy model with the easy axis aligned with the applied field, with $K = M_s B_c/2$ due to magnetization rotation (Morrish 1965; Cullity 1972). The formula, proposed initially for single domain (SD) grains (e.g. Stacey & Banerjee 1974) was latter also applied to larger grain were thehysteresis loops reach the reversible stage fully aligning the magnetization domains (Cullity 1972; Dekkers 1989b; Coey *et al.* 1995). This approach is similar to the calculations reported by Dekkers (1989b) and Coey *et al.* (1995).

The only difference is that here the saturation is measured whereas Dekkers (1989b) reported data the saturation state is extrapolated from the measurements.

Additionally, low temperature magnetization curves were measured with the PPMS magnetometer to identify the presence of hematite when concentration is too low to be detected by X-ray diffraction. Hematite is visible through the magnetic phase transition (Morin transition) at approximately 250 K (Morin 1950). At this temperature the spin structure changes from being confined within the basal plane to lying along the *c*-axis. Samples were cooled to 5 K in zero-field then warmed up to 400 K in a 100 mT field (ZFC curve). Subsequently, samples were cooled again to 5 K in a field of 1 and warmed up to 350 K in a 100 mT field (FC curve). Both ZFC and FC curves were measured in 4 K temperature steps. The maximum temperature reached was always below the transformation of goethite, which starts at 525 K (Francombre & Rooksby 1959).

3 RESULTS

3.1 Compositional analysis

X-ray diffraction confirms goethite as the main phase where the most prominent peaks from goethite have been identified with respected standard values (SLICE data file 01-081-0462). The powder used for the analysis has not been randomized and therefore broadening of the diffractograms lines can only be used as a pseudo-quantitative analysis of the crystallite size. Based on that, only sample GT5 shows a larger broadening of the spectrum that can be attributed a smaller crystallite size. The rest of the samples have very similar spectra. The presence of traces of hematite was revealed in four of the crystals with minor peaks slightly above the background signal (Table 1). Thermomagnetic curves allow the determination of the Néel temperature (T_N) of the goethite phases (Table 1 and Fig. 1). All the samples show very similar behaviour, identical to already reported thermoremanent curves on goethite single crystals (Özdemir & Dunlop 1996). The mean value of T_N = 102 °C is within the range of reported values (Szytuza *et al.* 1966; Özdemir & Dunlop 1996). Only sample GT3 has a value slightly lower.

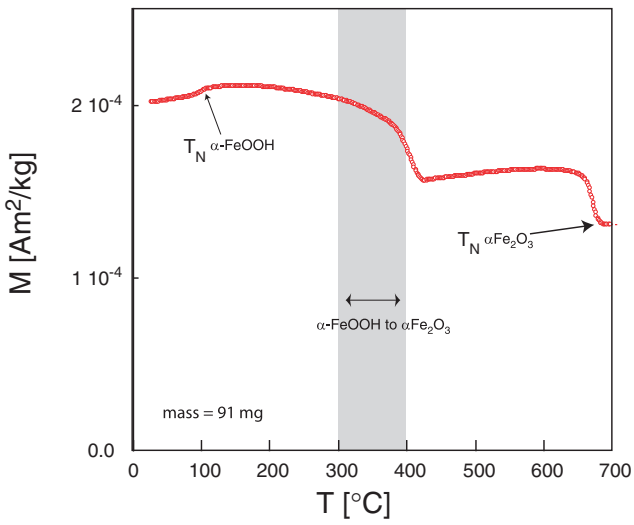

Figure 1. Representative thermomagnetic warming up run of a goethite single crystal (crystal GT2) indicating the Néel temperature of goethite, the dehydration range of goethite and the Néel temperature of hematite. The shading indicates the range of dehydration reaction.

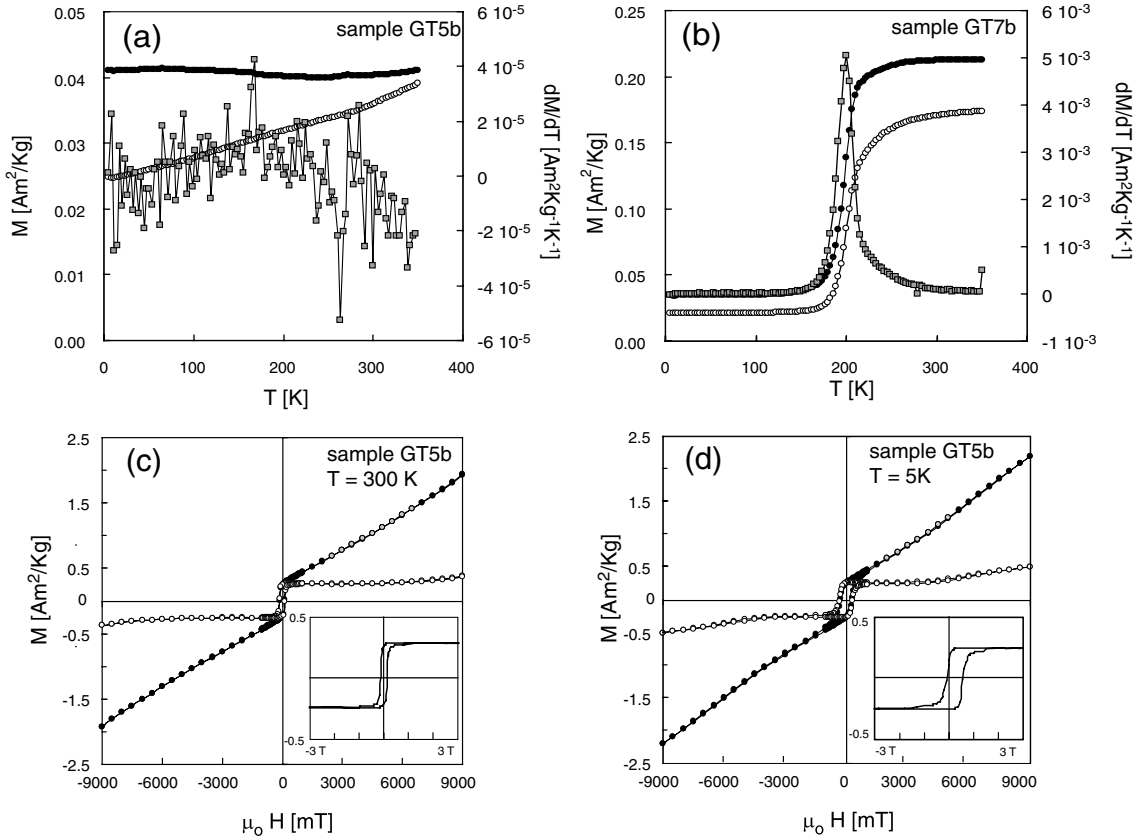

Figure 2. (a and b) Low-temperature magnetization measurements. Open circles correspond to the warming curve from 5 to 350 K in a 100 mT of the sample after being cooled down in ZFC. The black circles correspond to the warming curve from 5 to 350 K in a 100 mT field of the sample after being cooled down in a 1 T field (FC). The grey squares correspond to the derivate of the FC. (a) Sample GT5b where no evidence of hematite have been observed and (b) sample GT7b where a Morin transition has been observed. (c and d) Hysteresis loops in applied fields up to 9 T on sample GT5b. Black circles correspond to the actual measured data, grey circles correspond to data where saturation is assumed and have been used to compute the paramagnetic susceptibility slope, open symbols correspond to the hysteresis corrected by the paramagnetic slope. The inset shows the central part of the hysteresis loops after the paramagnetic slope correction. (c) Measurements at 300 K and (d) measurements at 5 K.

There are no significant variations in the Al, Ni, Co, Mn and Fe content between samples, only a larger value of the Mn content in samples were no hematite has been detected. The content of Al, a substituting cation that influences the magnetic properties of goethite (Liu *et al.* 2006), is almost constant (Table 1). Contrary to reported values based on Mossbauer spectroscopy (Pollard *et al.* 1991), the magnetic anisotropy is not influence by the Al content.

A drop in magnetization is also observed in the range of 250–400 °C (Fig. 1), which is attributed to the α-FeOOH dehydration that produces α-Fe_2O_3 in air (Francombre & Rooksby 1959; Dekkers 1988; Özdemir & Dunlop 1996). Finally, a total magnetization loss in the sample occurs at approximately 680 °C (Fig. 1), which is related to the Néel temperature of the newly formed hematite and the original hematite (Pollard *et al.* 1991; e.g. Dunlop & Özdemir 1997). It is difficult to distinguish between original and newly formed hematite, from a mass viewpoint the newly formed hematite will dominate but its magnetic moment is very, very small (e.g. Dunlop 1972; Dekkers 1990).

3.2 Low temperature remanence measurements

Samples can be classified into two groups according to the ZFC and FC curves. Samples where no evidence of hematite has been detected show a temperature-independent FC curve with increasing temperature and an increase in the ZFC curves with increasing temperature (Fig. 2a). Since no magnetic phase transition is observed, the derivative of the FC curve has no remarkable features (Fig. 2a). The second group shows evidence for hematite. Fig. 2(b) shows the ZFC and FC curves and the derivative of the FC, which exhibit a sharp increase in the magnetization crossing the magnetic phase transition associated to hematite, the Morin Transition (T_M) (Morin 1950). Table 1 summarizes the Morin transition in the samples where it has been observed, determined from the derivate of the FC curve. It compares well with reported data in the literature (Ozdemir *et al.* 2008). In general the results tend toward the lower limit, suggesting a small size of the hematite inclusions (Ozdemir *et al.* 2008 and references therein) and/or a pronounced ellipsoidal or rhombohedral shape (Mitra *et al.* 2009).

3.3 Room temperature hysteresis

Hysteresis loops reach the reversible state at fields ranging from 2 to 3 T (Fig. 2c and Table 2). Standard rock magnetic parameters derived from the hysteresis loops have the following mean value $M_s = 0.31 \pm 0.03$ Am^2 kg^{-1} and $B_c = 160 \pm 40$ mT. Both saturation magnetization and coercivity are consistent with reported values for goethite by magnetic methods (Hedley 1971; Dekkers 1989b; Dunlop & Özdemir 1997), although B_c values are slightly lower probably due to the large dimension of the crystals. Values of M_r/M_s ratio very close to 1, with a mean value of $M_r/M_s = 0.9 \pm 1$, confirm

Table 2. Mass in grams, main rock-magnetic parameters, mass saturation remanence (M_r), mass specific saturation magnetization (M_s), coercive force (B_c), asymmetry of the hysteresis with respect to the vertical axis (ΔB_c), M_r/M_s ratio and first anisotropy constant (K).

		Room temperature (300 K)						Low temperature (5 K)					
	Mass (g)	M_r (Am^2 kg^{-1})	M_s (Am^2 kg^{-1})	B_c (mT)	ΔB_c (mT)	M_r/M_s	K (J m^{-3})	M_r (Am^2 kg^{-1})	M_s (Am^2 kg^{-1})	B_c (mT)	ΔB_c (mT)	M_r/M_s	K (J m^{-3})
GT1a	0.0992	0.2819	0.3080	173.9	~	0.9155	114.29	0.0962	0.2067	579.3	7.0	0.4655	255.5
GT2a	0.2306	0.2719	0.3279	107.4	~	0.8293	75.12	0.0302	0.0866	2979.9	11.8	0.3491	550.7
GT2b	0.1331	0.2749	0.3461	96.7	~	0.7943	71.43	0.0287	0.2914	891.9	16.6	0.0984	554.6
GT3a	0.0931	0.2670	0.2958	166.7	~	0.9026	105.27	0.2865	0.2936	357.3	~	0.9759	223.8
GT3b	0.2215	0.2812	0.3023	175.7	~	0.9301	113.35	0.3118	0.3325	360.1	~	0.9378	255.5
GT4a	0.2780	0.2975	0.2974	208.6	~	1.0000	132.42	0.0349	0.3557	514.6	3.5	0.0980	390.7
GT4b	0.0681	0.2635	0.2894	210.2	~	0.9108	129.80	0.2346	0.3125	539.2	~	0.7506	359.6
GT5a	0.1762	0.2335	0.2613	124.6	~	0.8935	69.51	0.2493	0.2587	318.6	~	0.9634	175.9
GT5b	0.1640	0.2417	0.2626	123.6	~	0.9203	69.29	0.2589	0.2630	323.2	~	0.9846	181.3
GT7a	0.1541	0.3146	0.3309	154.2	~	0.9507	108.87	0.0349	0.3557	837.2	~	0.0980	635.6
GT7b	0.071	0.3004	0.3365	166.3	~	0.8925	119.41	0.0395	0.3448	1025.0	41.5	0.1145	754.2

Notes: All parameters have been determined at 300 and 5 K. Value of K have been normalized by volume using a mean value of $\rho = 4268$ kg m^{-3} (Lindsley *et al.* 1966).

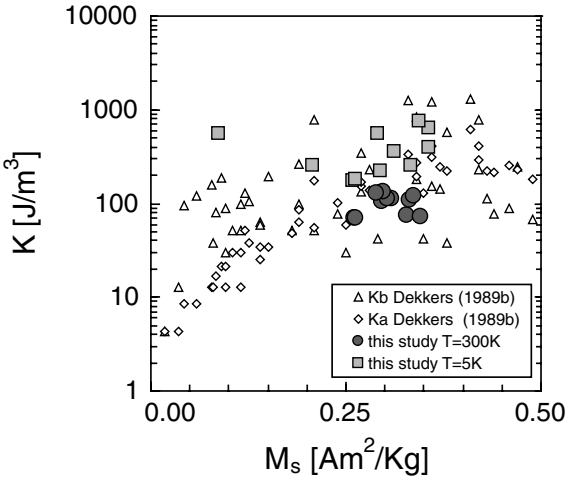

Figure 3. First anisotropy constant as a function of the saturation magnetization in goethite single crystals from this study and previously reported values. Dark circles correspond to single crystals from this study at 300 K, grey squares correspond to single crystals from this study at 5 K, open diamonds (Ka) and open triangles (Kb) correspond to already reported values at room temperature by Dekkers (1989b) using the formulas expressed by O'Reilly (1984) and Stacey & Banerjee (1974), respectively.

that samples are well-oriented along the crystallographic *c*-axis, the magnetic easy axis. The derived first anisotropy constant is well grouped (Table 2 and Fig. 3) and consistent with reported values of natural goethite fractions (Dekkers 1989b). A mean value of $K = 90 \pm 20$ Jm^{-3} has been evaluated for the pure goethite samples.

3.4 Low temperature hysteresis

Hysteresis loops reach the reversible state at fields ranging from 2 to 3 T, but in general at fields slightly higher than the corresponding room-temperature curves (Fig. 2d and Table 1). M_s has a mean value of $M_s = 0.28 \pm 0.08$ Am^2 kg^{-1}. B_c has a large scatter but when only the pure samples are considered an statistically significan mean value can be computed with $B_c = 340 \pm 20$ mT. Both M_r and M_s decrease whereas the coercivity B_c increases at 5 K. The ΔB_c, or shift of the hysteresis with respect to the vertical axes is related to the presence of exchange bias (Nogues & Schuller 1999). It is due to the intimate intergrown goethite and hematite or interaction between the weak ferromagnetic and antiferromagnetic phases of defective goethite (Barrero *et al.* 2006). This phenomenon can be neglected at room temperature because the obtained values are lower than the residual field of the instrument (1.2 mT). The hysteresis loops shows a significant shift with respect to the vertical axis (Table 2) for samples where hematite has been detected by other methods. This result suggests that origin is due to the presence of hematite and not interaction between ferromagnetic and antiferromagnetic phases.

The first anisotropy constant (K) has a large scatter (Table 2). The values can be divided in two groups, one group of four samples with well grouped and slightly higher than values at room temperature and the other group with higher values (Fig. 3). The first group coincides with samples where hematite has not been detected and therefore the scatter present in the second group is associated to the existence of hematite (Table 2). The mean value computed for samples with no evidences of hematite is 210 ± 40 Jm^{-3} at 5 K, smaller than the lower limit of 8000 Jm^{-3} estimated at 4.2 K by Coey *et al.* (1995).

4 DISCUSSION AND CONCLUSIONS

4.1 Rock magnetic properties

The thermomagnetic curves shows that there are variations in the Néel temperature that can be attributed to vacancy defects (Bocquet & Kennedy 1992) or substitution (Pollard *et al.* 1991). The possibility of differences in the crystallite size can be excluded because the only sample where X-ray diffractograms show a broadening in the lines is GT5, which has a $T_N = 119°C$. The sample with lower Neel temperature is GT3 and can be attributed to a larger Mn content. The presence of Mn into the goethite lattice has been suggested to lower the Neel temperature, but the mechanism is not well known (Vempati *et al.* 1991). A third possibility could be an excess of water content, which also has been reported to low the Neel temperature (Betancur *et al.* 2004; Barrero *et al.* 2006). Further analysis using mass loss techniques would be required to prove this third hypothesis.

The inflection point associated with the dehydration reaction of goethite within reported values. The starting point starts at temperature between 200 and 220 °C. This ranges has been reported to be influence by crystallinity, substitutions and water content (Dekkers 1990). However the final temperature is in all samples at about 400 °C, therefore no information about crystallites size and/or water can be inferred from the thermomagnetic curves. The temperature at which the reaction starts has been found to be independent of the heating rate (repeating the experiment in 40 and 10 °C min^{-1} rate gives the same T range).

The M_r/M_s ratio is very close to 1, confirming the c-axis alignment and validity of the uniaxial model of magnetic anisotropy (Cullity 1972). It the material is supposed to be purely antiferromagnetic, the hysteresis loop will be a squared loop and $M_r/M_s = 1$. The deviation angle can be attributed to a missorientation effect. Assuming $M_r/M_s = \cos(\theta)$ the deviation angle can be estimated for the measurement giving a mean value of 24° at room temperature. However, this effect does not seem to be the only reason because when the same model is proposed to the low temperature measurements, the angle can reach 80°. Other authors have reported that goethite orders in a non-collinear four sublattice of antiferromagnetic structure, with a canting angle of 13° (Coey *et al.* 1995). The ordering of the magnetic domain structures and the deviation from the pure uniaxial model of magnetic anisotropy is suggested to contribute to this effect.

This work is based on the empirical result of reversible behaviour of the magnetic hysteresis reached at 2–3 T. This result is in apparent inconsistency with the hard remanent magnetization of some natural goethite samples and goethite rich sediments, which failed reaching saturation at 57 T (Rochette *et al.* 2005) or 9 T (Walden *et al.* 2000). However the difference in crystallite size and thus zero-field domain state is at the root of the apparent inconsistency. It has been shown that a strong relationship between grain size and magnetic properties exist for goethite. The underlying idea is that not only grain size but also the interaction between goethite crystallites and their size (Dekkers 1989b).

Low temperature ZFC–FC curves detect the presence of a magnetic transition in the range of 200–250 K, which has been attributed to hematite Morin transition (Morin 1950). The values are slightly lower than the standard 250 K (c.f., Dunlop & Özdemir 1997). However it has been shown that Morin transition decreases with decreasing grain size until it is reached a minimum size of 20 nm in which it is suppressed (Jacob & Khadar 2010). This suggests that the hematite particles grown in the goethite crystals are of very small size.

4.2 Anisotropy constant

A mean value of 90 ± 20 Jm^{-3} has been determined for the magnetic anisotropy constant at room temperature using only those samples where no hematite has been detected. This estimation is two orders of magnitude smaller than that based on Mössbauer spectroscopy, which is approximately 5×10^4 Jm^{-3} (Pankhurst & Pollard 1990; Coey *et al.* 1995; Madsen *et al.* 2009). The obtained values agree with previously reported values based on hysteresis parameters (Dekkers 1989b). The main advantage of our results with respect to previous data is that we ensure we have reached reversible behaviour, therefore we can assume a purely uniaxial hysteresis loop. Previously reported data use the estimation of K for SD particles extrapolated to the reversible state. Here the reversible state is measured empirically. Deviations between the measured and extrapolated values might be a reason for the differences. Independently of the method used, our data lie on the larger grain size fraction, compatible with the expected domain structure of a macroscopic crystal.

The mean value of the first anisotropy constant at low temperature for the pure goethite samples is $K = 210 \pm 40$ Jm^{-3}. Few authors have reported low temperature estimations of the anisotropy constant based on magnetometry measurements, but a value of 8×10^3 Jm^{-3} has been considered a lower limit boundary using this technique (Coey *et al.* 1995). From our measurements an increase in the anisotropy constant is observed, which is also observed in Mössbauer estimations despite the different obtained value (Madsen *et al.* 2009).

The origin of the discrepancy lies in the different relaxation times associated with Mössbauer and magnetometry. The timescale for a Mössbauer experiment on goethite samples is in the order of $\sim 10^{-8}$s and a correlation time for the nucleus fluctuation of 10^{-11} to 10^{-12} s (Bocquet *et al.* 1992). However, the timescale for a magnetic hysteresis experiment is in the order of 10–100 s and the relaxation time can be considered as 10^{-9} s, which is atomic reorganization time (Dunlop & Özdemir 1997). This is the underlying reason for the disagreement between the two techniques. For this reason, when models of magnetization acquisition, FORC diagram description or micromagnetic models are presented on goethite or goethite bearing rocks, the corresponding K value obtained by magnetic methods must be used.

ACKNOWLEDGMENTS

We kindly acknowledge revision of the manuscript by G. McIntosh and M.J. Dekkers and one anonymous reviewer for the valuable suggestions. The paper has benefit from the help by the X-ray Center and Dr. Mayte Larrea from the Resarch Assistance Spectrometry Center from the UCM. This work has been supported by the "Ramón y Cajal" research project to FMH and project MAT2008-06517-c02-01 to MMGH (both from the Spanish Ministry of Science).

REFERENCES

Balsam, W., Ji, J. & Chen, J., 2004. Climatic interpretation of the Luochuan and Lingtai loess sections, China, based on changing iron oxide mineralogy and magnetic susceptibility, *Earth planet. Sci. Lett.,* **223,** 335–348.

Banerjee, S.K., 1970. Origin of thermoremanence in goethite, *Earth planet. Sci. Lett.,* **8,** 197–201.

Barrero, C.A., Betancur, J.D., Greneche, J.M., Goya, G.F. & Berquo, T.S., 2006. Magnetism in non-stoichiometric goethite of varying total water content and surface area, *Geophys. J. Int.,* **164,** 331–339.

Betancur, J.D., Barrero, C.A., Greneche, J.M. & Goya, G.F., 2004. The effect of water content on the magnetic and structural properties of goethite, *J. Alloys Comp.,* **369,** 247–251.

Bibring, J.P. *et al*., 2007. Coupled ferric oxides and sulfates on the martian surface, *Science,* **317,** 1206–1210.

Bocquet, S. & Kennedy, S.J., 1992. The Néel temperature of fine particle goethite, *J. Magn. Magn. Mater.,* **109,** 260–264.

Bocquet, S., Pollard, R.J. & Cashion, J.D., 1992. Dynamic magnetic phenomena in fine-particle goethite, *Phys. Rev. B,* **46,** 11657–11664.

Coey, J.M.D., Barry, A., Brotto, J.M., Rokoto, H., Brennan, S., Mussl, W.N., Collomb, A. & Fruchart, D., 1995. Spin flop in goethite, *J. Phys. Condens Matter,* **7,** 759–768.

Cullity, B.D., 1972. *Introduction to Magnetic Materials,* Addison-Wesley, Reading, MA, 666 pp.

Dekkers, M.J., 1988. Magnetic behavior of natural goethite during thermal demagnetization, *Geophys. Res. Lett.,* **15,** 538–541.

Dekkers, M.J., 1989a. Magnetic properties of natural goethite. Part II. TRM behaviour during thermal and alternating field demagnetization and low-temperature treatment, *Geophys. J. Int.,* **97,** 341–355.

Dekkers, M.J., 1989b. Magnetic properties of natural goethite. Part I. Grain-size dependence of some low- and high-field related rock magnetic parameters measured at room temperature, *Geophys. J. Int.,* **97,** 323–340.

Dekkers, M.J., 1990. Magnetic properties of natural goethite. Part III. Magnetic behaviour and properties of minerals originating from goethite dehydration during thermal demagnetization, *Geophys. J. Int.,* **103,** 233–250.

Dekkers, M.J. & Rochette, P., 1992. Magnetic properties of chemical remanent magnetization in synthetic and natural goethite: prospects for a natural remanent magnetization/thermoremanent magnetization ratio paleomagnetic stability test? *J. geophys. Res. B: Solid Earth,* **97,** 17 291–17 307.

Dunlop, D.J., 1972. Magnetic mineralogy of unheated and heated red sediments by coercivity spectrum analysis, *Geophys. J. R. astr. Soc.,* **27,** 37–55.

Dunlop, D.J. & Özdemir, Ö., 1997. *Rock Magnetism: Fundamentals and Frontiers*. Cambridge Studies in Magnetism, Cambridge University Press, Cambridge, 573 pp.

Evans, M.E. & Heller, F., 2003. *Enviromental Magnetism: Principles and Applications of Enviromagnetics,* International Geophysics Series, 86. Accademic Press, London, 299 pp.

Francombre, M.H. & Rooksby, H.P., 1959. Structure transformations effected by the dehydration of diaspore, goethite and delta ferric oxide, *Clay Min. Bull.,* **4,** 1–14.

Hedley, I.G., 1971. The weak ferromagnetism of goethite (α-FeOOH), *Zeitschrift für Geophysik,* **37,** 409–420.

Jacob, J. & Khadar, M.A., 2010. VSM and Mossbauer study of nanostructured hematite, *J. Magn. Magn. Mater.,* **322,** 614–621.

Lindsley, D.H., Andreasen, G.E. & Balsley, J.R., 1966. Magnetic properties of rocks and minerals, in *Handbook of Physical Constants,* pp. 543–552, ed. Clark, S.P., Geological Society of America, New York.

Liu, Q., Yu, Y., Torrent, J., Roberts, A.P., Pan, Y. & Zhu, R., 2006. Characteristic low-temperature magnetic properties of aluminous goethite [α-(Fe,Al)OOH] explained, *J. geophys. Res.,* **111,** doi: 10.1029/2006JB004560.

Madsen, D.E., Cervera-Gontard, L., Kasama, T., Dunin-Borkowski, R.E., Koch, C.B., Hansen, M.F., Frandsen, C. & Morup, S., 2009. Magnetic fluctuations in nanosized goethite (α-FeOOH) grains, *J. Phys. Condens Matter,* **21**(1), 1–11.

Maher, B.A., Karloukovski, V.V. & Mutch, T.J., 2004. High-field remanence properties of synthetic and natural submicrometre haematites and goethites: significance for environmental contexts, *Earth planet. Sci. Lett.,* **226,** 491–505.

Meagher, A., Pankhurst, Q.A. & Dickson, D.P.E., 1986. A Mössbauer spectroscopy study of the magnetocristalline anisotropy in α-FeOOH, *Hyperfine Interact.,* **28,** 533–536.

Mitra, S., Das, S., Basu, S., Sahu, P. & Mandal, K., 2009. Shape- and field-dependent Morin transitions in structured [alpha]-Fe2O3, *J. Magn. Magn. Mater.,* **321,** 2925–2931.

Morin, J., 1950. Magnetic susceptibility of α-Fe_2O_3 and Fe_2O_3 with added titanium, *Phys. Rev.,* **78,** 819–820.

Morrish, A.H., 1965. *The Physical Principles of Magnetism,* John Wiley, New York, 680 pp.

Mørup, S., 1990. Mössbauer effect in small particles, *Hyperfine Interact.,* **60,** 959–973.

Nogues, J. & Schuller, I.K., 1999. Exchange bias, *J. Magn. Magn. Mater.,* **192,** 203–2032.

O'Reilly, W., 1984. *Rock and Mineral Magnetism,* Blackie, Glasgow, 230 pp.

Ozdemir, O., Dunlop, D.J. & Berquo, T.S., 2008. Morin transition in hematite: size dependence and thermal hysteresis, *Geochem. Geophys. Geosyst.,* **9,** doi: 10.1029/2008gc002110.

Özdemir, Ö. & Dunlop, D.J., 1996. Thermoremanence and Néel temperature of goethite, *Geophys. Res. Lett.,* **23,** 921–924.

Pankhurst Q.A. & Pollard, R.J., 1990. Mossbauer spectra of antiferromagnetic powders in applied fields, *J. Phys. Condens. Matter,* **2,** 7329–7337.

Pollard, R.J., Pankhurst, Q.A., & Zientek, P., 1991. Magnetism in aluminous goethite, *Phys. Chem Minerals,* **18,** 259–264.

Rochette, P. & Fillion, G., 1989. Field and temperature behavior of remanence in synthetic goethite: paleomagnetic implications, *Geophys. Res. Lett.,* **16,** 851–854.

Rochette, P., Jackson, M. & Aubourg, C., 1992. Rock magnetism and the interpretation of anisotropy of magnetic susceptibility, *Rev. Geophys.,* **30,** 209–226.

Rochette, P., Mathe, P.E., Esteban, L., Rakoto, H., Bouchez, J.L., Liu, Q. & Torrent, J., 2005. Non-saturation of the defect moment of goehtite and fine-grained hematite up to 57 teslas, *Geophys. Res. Lett.,* **32,** L2239, doi: 10.1029/2005GL024196.

Stacey, F.D. & Banerjee, S.K., 1974. *The Physical Principles of Rock Magnetism,* Elsevier, Amsterdam, 195 pp.

Szytuza, A., Burewicz, A., Dyrek, K., Hrynkiewicz, A., Kulgawczuk, D., Obuszko, Z., Rzany, H. & Wanic, A., 1966. Susceptibility measurements of the antiferromagnetic α-goethite, *Phys. Stat. Sol.,* **17,** K195–K197.

Vempati, R.K., Morris, R.V. & Lauer, H.V., 1991. Effect of Mn substitution on the spectral properties of goethites and hematites, in *Proceedings of the Abstracts of the Lunar and Planetary Science Conference,* Vol. **22**, 1437 pp.

Walden, J., White, K.H., Kilcoyne, S.H. & Bentley, P.M., 2000. Analyses of iron oxide assemblages within Namib dune sediments using high field remanence measurements (9 T) and Mossbauer analysis, *J. Quat. Sci.,* **15,** 185–195.